PAPER

CrossMark
← click for updates

Aromatic polyamides and acrylic polymers as solid sensory materials and smart coated fibres for high acidity colorimetric sensing†

Miriam Trigo-López, Jesús Luis Pablos, Asunción Muñoz, Saturnino Ibeas, Felipe Serna, Félix Clemente García and José Miguel García*

Reusable colorimetric acid responsive coated fibres and manageable films or membranes have been successfully designed and prepared herein. The design of the materials rely on the preparation of condensation and addition monomers both having the azobenzene group, which is used as a dye moiety and as a weak basic motif, and a *N,N*-dimethylamino moiety. The *N,N*-dimethylamino moiety is also used as a weak, albeit stronger, basic group as well as an electron donor or electron withdrawal group, depending on its protonation state. For the sake of applicability, the coated fibres were cotton commodity fabrics, and high-tech aromatic polyamide yarns and fabrics. The high-performance aromatic polyamides and the versatile acrylic structures, along with the pendant weak basic groups, with pK_as in water ranging from 1.78 to −0.5 and in air from −1.5 to −3.9, provide the materials with a colorimetric sensing capability over a wide acidity sensing window. This sensing window ranges from 1×10^{-2} to 3 M for perchloric acid in water and from 4×10^{-7} to 9×10^{-2} atm for vapour pressure of hydrogen chloride in air. The colour change of the sensory materials from yellow/blank to red or purple, which occurs upon contact with acidic media, was easily identified using the naked eye. Washing these materials with pure water recovered their original colour and permitted their reuse.

Introduction

Precise control over the acidity or basicity of different media is fundamental in chemical, cosmetic and household industries; for environmental control and remediation; and in life sciences. Acidity or basicity in aqueous media is usually monitored using the standard pH scale, which ranges from 1 to 13,[1] by different techniques that perform well in covering most of the laboratory requirements. The most popular and easy to use method is that of using pH test paper strips, followed by potentiometric techniques based on a proton sensitive membrane, such as a glass membrane electrode. Less extensively used are chemical pH sensors.[2–4]

For the same reasons, there is a huge need for controlling the acidity or basicity of systems not within range of this scale,

Departamento de Química, Facultad de Ciencias, Universidad de Burgos, Plaza de Misael Bañuelos s/n, 09001 Burgos, Spain. E-mail: jmiguel@ubu.es;
Fax: (+) 34 947 258 831; Tel: (+) 34 947 258 085

†Electronic supplementary information (ESI) available: Experimental part (intermediate, monomer and material characterization, correlation between the acidity function (H_0) and the concentration of perchloric acid, titration of perchloric acid, titration of HCl vapours, pK_1 of monomer (3) and model (5) calculated by ^{1}H NMR, response time, and interference study). See DOI: 10.1039/c4py01545b

both in strongly acidic or basic aqueous media as well as in the environment – in air – where the pH scale is not applicable. This need is especially relevant for a number of important social and economic applications, including work related to the separation of rare-earth metals, nuclear fuel reprocessing, and the recycling and reuse of strong acids in industrial processes.[5–10] Within this frame, we describe herein colorimetric sensory polymers, which have in their pendant structure azo and amino groups, which are used both as proton receptors and chromogenic moieties. These groups change their colour in highly acidic aqueous media and in air, providing a rapid, precise, and inexpensive measure of the acidity at very low pH values, specifically values outside of the standard pH scale (perchloric acid concentration up to 3 M can be detected). These polymers have a high-performance aromatic polyamide main structure[11–14] or an acrylic nature with gel behaviour,[15–18] which can be prepared or transformed into highly manageable materials including films, membranes, or coatings for cotton commodity or high-tech *meta*- or *para*-aromatic polyamide fibres. To date, the challenge of preparing pH-responsive polymeric materials has been mainly undertaken by immobilising pH responsive organic molecules in polymer matrixes[7,8–10,19,20] with only few studies on the preparation of integral polymer chemosensors.[6,21] However, the

latter approach proved to be better[22,23] than the former[24–30] because the chemical anchoring of the sensory motifs avoids the migration, leaching and hysteresis of any sensory material, thus giving rise to an unsurpassed long-term stability. However, although azobenzene polymers have been used as photo- and pH-responsive nanoparticles or hydrogels[31–33] due to their well-known *cis–trans* thermal- and photo-isomerisation and dependence on the medium acidity,[34–36] to the best of our knowledge, this kind of material has not been fully exploited. Further exploitation includes taking advantage of the colorimetric behaviour of manageable films and coated fibres, which is due to the protonation process of the azo group and more precisely to the two protonation processes corresponding to the 4-dimethylaminoazobenzene dye moiety. These processes have reported second acidity constants (protonation of the azo group) ranging from −4.4 to −3.4 with a first acidity constant (protonation of the amino group) of approximately 3.5.[37,38]

Thus, we have designed sensory condensation and acrylic monomers from which we have prepared colorimetric sensory materials that respond to acidic environments, both in aqueous solutions and in air, with a clearly visible colour change. For the correct design of colorimetric acidity-responsive materials, the acidity constants of the proton receptors of the monomers were previously considered, along with both the chromogenic and weak basicity of the azobenzene moiety. As a proof of concept for practical applications, the materials have been prepared as manageable transparent membranes (shaped as films), coated fibres of cotton fabrics, and *meta*- and *para*-aromatic polyamide yarns and fabrics (commercial brands: Nomex®, Teijinconex®, and Kevlar®, Twaron®, respectively).

Experimental part

Instrumentation and measurements

^{1}H and ^{13}C NMR spectra were recorded using a Varian Inova 400 spectrometer operating at 399.92 and 100.57 MHz, respectively, with deuterated dimethylsulphoxide (DMSO-d_6) as the solvent.

Infrared spectra (FT-IR) were recorded using a FT/IR-4200 FT-IR Jasco spectrometer with an ATR-PRO410-S single reflection accessory. Low-resolution electron impact mass spectra (EI-LRMS) were obtained at 70 eV on an Agilent 6890N mass spectrometer. Thermogravimetric analysis (TGA) data were recorded for a 5 mg sample under a nitrogen or oxygen atmosphere on a TA Instrument Q50 TGA analyser at a scan rate of 10 °C min^{-1}. The limiting oxygen index (LOI) was estimated using the following experimental Van Krevelen equation: LOI = 17.5 + 0.4 CR, where CR is the char yield weight percentage at 800 °C, which was obtained from the TGA measurements under a nitrogen atmosphere.

UV/Vis spectra were recorded using a Varian Cary3-Bio UV/Vis spectrophotometer.
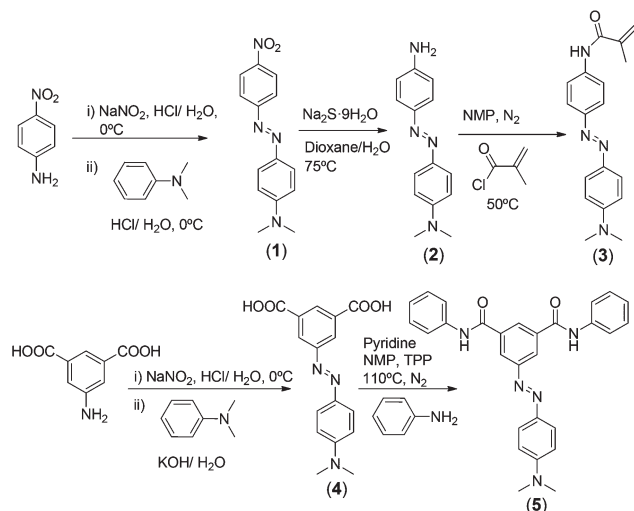
The polyamide solubility was determined by mixing 10 mg samples of **PA1** and **PA2** with 1 mL of a solvent followed by stirring for 24 h at 20 °C. The polymer was considered to be soluble at room temperature if a homogeneous solution was obtained. If the polymer was insoluble at room temperature, the system was heated to reflux for 2 h, and the polymer was considered to be soluble on heating if a homogeneous solution was obtained. Otherwise, the polymer was considered to be insoluble. The inherent viscosities of the polymer were measured with an Ubbelohde viscometer using sulphuric acid (96%) and NMP as the solvents at 25 °C ± 0.1 °C and a polymer concentration of 0.5 g dL^{-1}.

Water sorption experiments were conducted gravimetrically. The sample (200 mg) was dried at 60 °C for 24 h over phosphorus pentoxide, and the sample was placed in a closed box containing a saturated aqueous solution of $NaNO_2$ at 20 °C, which provided a relative humidity of 65%. The samples were weighed periodically over a period of 8 days until they equilibrated with their surroundings and presented no further changes in weight. The water-swelling percentage (WSP) of the membranes or films was obtained from the weights of a dry sample membrane (ω_d) and a water-swelled (the membrane was immersed in pure water at 20 °C until the swelled equilibrium was achieved) sample membrane (ω_s) as follows: 100 × $[(\omega_s - \omega_d)/\omega_d]$.

Polyamide films were prepared by evaporation of cast solutions in DMA: solutions 4% by polymer weight for **PA1** and 10% by polymer weight for **PA2** were used. The solvent was eliminated by heating at 60 °C overnight. The polymethacrylamide membrane or film, **M1**, was prepared by bulk radical polymerization as described in the ESI (section S2†). To determine the tensile properties of the polyamides, strips (5 mm in width and 30 mm in length) were cut from polymer films of 22 and 71 μm thicknesses for **PA1** and **PA2**, respectively, on a Shimadzu EZ Test Compact Table-Top Universal Tester at rt. Mechanical clamps were used and an extension rate of 5 mm min^{-1} was applied using a gauge length of 9.44 mm. The polymethacrylamide membrane, **M1**, 112 μm in thickness, was also tested in the same way. At least 6 samples were tested for each polymer, and the data were then averaged.

The acid titration monitored by UV/Vis both for the vapour and in aqueous phases was performed as follows. The titration in solution with the sensory membranes was performed using perchloric acid as the acid source using the following conditions: 5 mm discs cut from membrane **M1** and casted films of **PA1** were dipped into 200 mL of water (Millipore-Q) using a homemade support that also fit the UV/Vis cell holder. Next, the acidity of the solution was increased to a pH close to 1 by adding aliquots of diluted perchloric acid. After each addition, the pH was measured using a pH meter with a glass electrode, the membranes were allowed to equilibrate for 15 min, and the UV/Vis spectra were recorded. For higher acidities out of the range of the pH scale, vials containing 25 mL of perchloric acid of concentrations ranging from 0.1 to 3.5 M were prepared, and the membranes were successively immersed in them, starting from the lower acid concentration vial. After

Scheme 1 Synthesis of monomers (**3** and **4**) and model (**5**).

equilibrating the three films or membranes in each vial for 15 min, their UV/Vis spectra were recorded. The measurements were performed at 25 °C. The colorimetric detection of acidic vapours was performed quantitatively as follows. The HCl vapour pressure of vapours from the head space of a fresh bottle of concentrated hydrochloric acid was calculated by titration with NaOH solution of known concentration. The titration was repeated five times and the results averaged. The membranes (**PA1** casted films and 5 mm discs cut from **M1**) were placed in a sealed quartz UV-cuvette using a homemade support. Then, increasing volumes of HCl vapours from the head space of the bottle were then added with a Hamilton micro syringe, and the UV/Vis spectra were recorded after equilibrium (see the Response time subsection). The measurements were performed at 25 °C.

Synthesis of sensory monomers and preparation of sensory materials

Monomers and polyamide models were prepared by previously described procedures schematically depicted in Scheme 1 (for experimental workup see section S1, ESI†).[39–41] The aromatic polyamide synthesis (**PA1** and **PA2**, Scheme 2), the crosslinked acrylic membrane preparation (**M1**, Scheme 2) and the coating of cotton and aramid fibres with the acidity sensory polymers (Table 1) were carried out following previous methodologies (see section S2, ESI†).[11,16,18,42,43]

Results and discussion

Overcoming the difficulty of sensing target molecules in pure water and in the gas phase

Organic molecules usually are water-insoluble and can barely be exploited in water media. Furthermore, the lack of mechanical properties of discrete molecules also impairs their applicability. Our main objective is sensing target molecules in water

easily, *i.e.*, using inexpensive and manageable solid systems that rapidly change their colour *in situ* upon interacting with the target in aqueous media, and that can be used by non-specialised personnel. For this purpose, we have designed organic probes that change their colour when exposed to different levels of acidity. Furthermore, the probes are aromatic diacids and acrylic monomers that allow for their polymerisation to render solid, handleable materials (as films or membranes) and coated fibres (both for use in commodity and high-tech smart textiles). Simultaneously, the copolymerisation of the probes with the suitable monomers provides a macromolecular environment for sensing in water regardless of the water insolubility of the probes. The change of the colour of the materials is clearly visible at given acid concentrations, permitting the broad determination of their acidities using the naked eye, which can be quantified in parallel using the UV/Vis technique. Furthermore, the materials change their colour in air in the presence of acid vapours, allowing for use of these materials in the preparation of coated fibres that could be used in EPP (personal protective equipment).

The strategy followed for the design of the colorimetric chemosensory units

The design of a colorimetric sensory motif for acidic media relies on a highly conjugated system that provides the chromophore and link to an electron rich group capable of interacting with protons, preferably by being protonated. Protonation would then cause variation in the electron density of the conjugated sub-structure and, macroscopically, in the colour of the system.
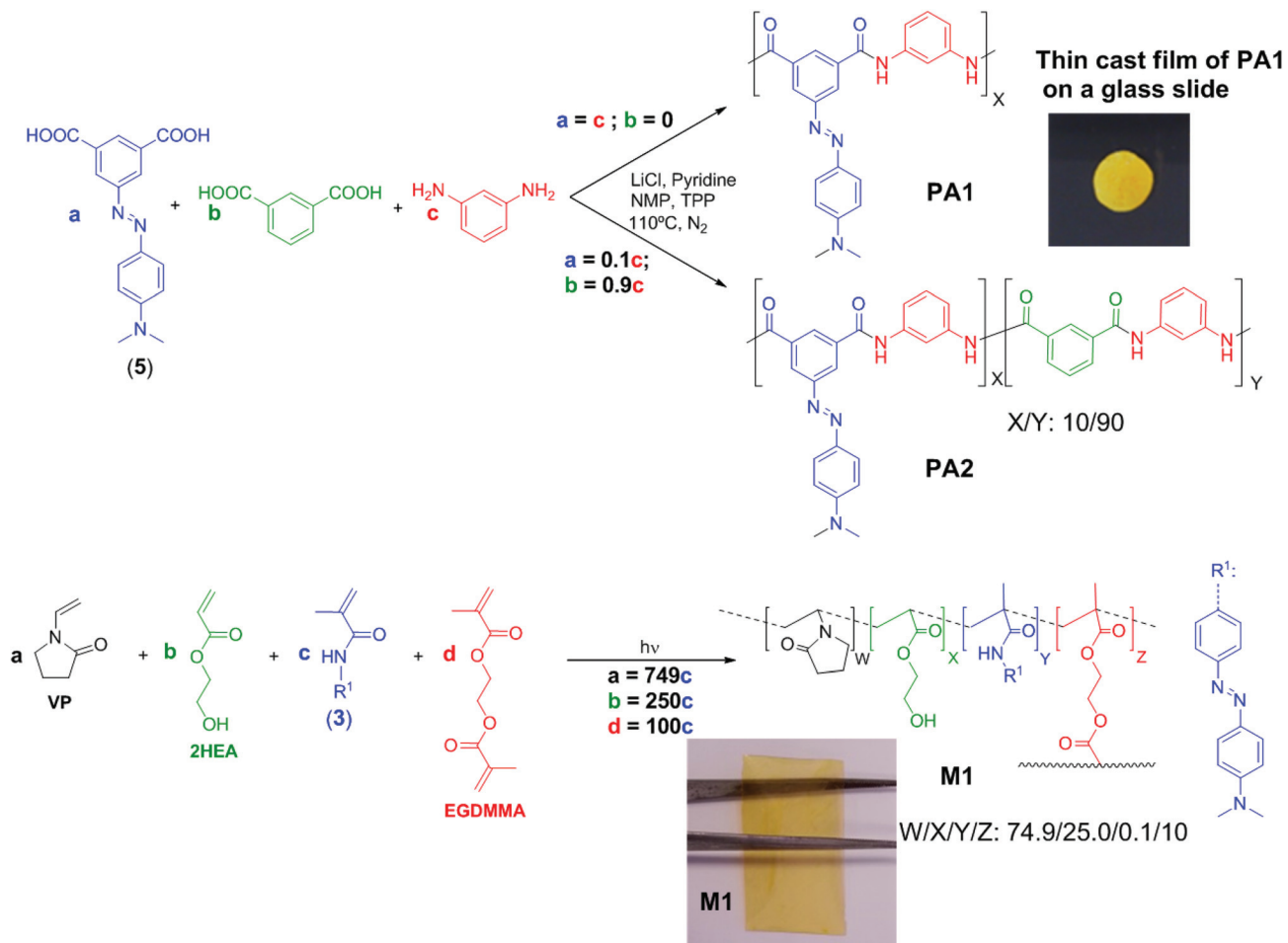
In this study we have chosen an azo dye for two reasons: (a) diazobenzene derivatives already have well-known dye characteristics, and (b) the azo group is a weak base that can be protonated.[36]

Moreover, the *N,N*-dimethylamino group, which is a stronger but still weak base, was chosen as a substituent at the *para* position of the 4-azobenzene ring. This group was chosen with the aim of using it as a primary protonation site at low pH and the azo motif as a second protonation site at an even lower pH as a way of expanding the acidity sensory range.

Material preparation and characterisation

Both the sensory acrylic and condensation monomers, (**3**) and (**4**), respectively, were prepared easily and inexpensively in several high-yield synthetic steps using widely available chemicals in proven organic reactions (Scheme 1). The ^{1}H and ^{13}C NMR and FTIR data and the spectra of the intermediates and monomers can be found in the ESI, section S1.† The potential applicability of the designed polyacrylic sensory membrane, **M1**, and even of the coating for commercial fibres, is highlighted by the fact that only 0.1% by weight of the sensory synthetic monomer is used in the preparation of the acid sensory materials, as will be described below, using 99.9 mol% of very inexpensive commercial comonomers. In a similar fashion, the sensory aromatic polyamides can be used to create an *m*-aramid-like structure as a homopolymer (**PA1**) or as a copoly-

Scheme 2 Polymer structure and synthesis.

Table 1 Polyamide (**PA1**) and polyacrylic coated fibres, and visual sensing behaviour toward acid vapours
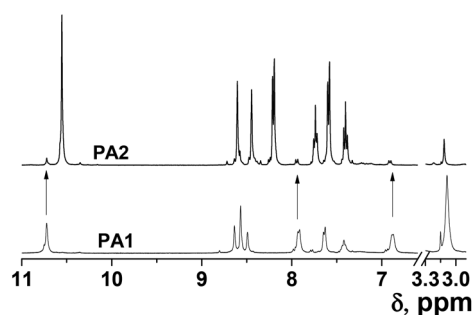
	Polyamide coating (**PA1**)			Polyacrylic coating		
	Blank fibres	Coated fibres and coating[a] (%)	HCl vapour	Blank fibres	Coated fibres and coating[a] (%)	HCl vapour
Cotton fabric		0.4			96	
m-Aramid yarns		1.2			674	
p-Aramid fabric		1.5			121	
p-Aramid yarns		1.6			321	

[a] Percentage of weight regain of blank samples upon coating.

Table 2 Viscosity, water sorption and solubility of materials

Model or polymer	$\eta_{inh}{}^a$ (dL g^{-1})	$\eta_{inh}{}^b$ (dL g^{-1})	Water sorption %^{c}	%^{d}	Solubility^e DMSO, DMA, DMF	NMP	THF	CHCl$_3$, CH$_2$Cl$_2$, EtOH	Acetone
Model	n.a.	n.a.	n.a.	n.a.	++	++	++	+	++
PA1	2.25	0.78	11	19	++	+	–	–	–
PA2	1.29	0.50	12	21	++	++	–	–	–
M1	n.a.	n.a.	37	53	n.a.	n.a.	n.a.	n.a.	n.a.

^{a} Solvent = sulphuric acid (96%), temperature = 25 °C, polymer concentration = 0.5 g dL^{-1}; n.a.: not applicable. ^{b} Solvent = NMP, temperature = 25 °C, polymer concentration = 0.5 g dL^{-1}; n.a.: not applicable. ^{c} Polymeric samples in an atmosphere with a relative humidity of 65%; n.a.: not applicable. ^{d} The water-swelling percentage (WSP) of membranes in pure water at 20 °C. ^{e} Polymer concentration = 10 mg of polymer in 1 mL of solvent; ++ = soluble at room temperature; + = soluble on heating; +– = partially soluble; – = insoluble, n.a.: not applicable (crosslinked membranes).

Fig. 1 ^{1}H NMR of **PA1** and **PA2** (solvent = DMSO-d$_6$).

mer (**PA2**) using 10% by weight of the diacid sensory monomer (**5**). The inherent viscosity of the polymers was high enough to assure their high molecular weight, and their solubility good to allow their processability upon solution (Table 2). Furthermore, using a coating lower than 2% by weight, for conventional cotton and high-tech aramid fibres, smart textiles were successfully tested. The structure of the homopolymer and of the copolymer, especially considering the molar content of the sensory motifs, was in agreement with the ^{1}H NMR spectra (Fig. 1).

The polymer dense membranes, or films, were characterised as materials from both mechanical and thermal viewpoints. Mechanically, they were creasable and handleable:

both for cast aromatic polyamide films prepared from **PA1** and **PA2** and for acrylic membrane **M1**. The aramids exhibited worthy Young's moduli and tensile strength for high-performance polymer films prepared at a laboratory scale without orientation and post-thermal treatment (Table 3). In the same fashion, these properties were also excellent when testing the acrylic membrane.

From the thermal resistance viewpoint, evaluated using TGA, the decomposition temperatures that resulted in a 5% weight loss under a nitrogen atmosphere (T_5) were approximately 330–400 °C for aromatic polyamides and approximately 320 °C for **M1**. The T_5 of the aromatic homopolyamide **PA1** was low for this type of material[11,12] due to the weight loss associated with the thermal degradation of the pendant azo group. Significantly, the LOI of aramids was high, which corresponds to the properties of high-thermal resistance materials (Table 3).

The films and membrane composition were designed to provide a high thermal, chemical and mechanical resistance in the case of polyamides (with a relatively high water affinity provided by the polar amide groups) and high hydrophilicity in the case of the crosslinked acrylic material (**M1**), *i.e.*, gel behaviour. This allows the solvated hydrated protons, hydronium ions, to enter the membrane by diffusion and to reach and interact with the hydrophobic sensory motifs evenly distributed along the swelled membrane. The hydrophilic or hydrophobic character of the membranes is related to water sorption,

Table 3 Thermal (TGA) and mechanical properties of materials

Polymer	Thermal properties N$_2$ atmosphere $T_5{}^a$ (°C)	$T_{10}{}^b$ (°C)	Char yield (%)	O$_2$ atm. $T_5{}^a$ (°C)	$T_{10}{}^b$ (°C)	LOI^c	Mechanical properties Tensile strength (MPa)	Young's modulus (GPa)	Elongation (%)
PA1	330	360	50	330	400	37.5	60	1.54	13
PA2	400	456	64	412	464	43.1	50	1.34	11
M1	319	367	6	292	353	19.9	22	0.83	4

^{a} 5% weight loss (T_5), 10% weight loss (T_{10}). ^{b} At 800 °C. ^{c} Limiting oxygen index, calculated from the TGA data (LOI = 17.5 + 0.4 CR, where CR is the char yield in% weight at 800 °C under nitrogen).
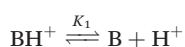
i.e., the moisture uptake at 65% RH in polyamide films, and to the water-swelling percentage (WSP) in acrylic membranes (that is, its character is related to the weight percentage of water uptake by the films upon soaking until equilibrium in pure water at rt). These data are shown in Table 2, which, thus, confirms the properties for which they were designed.

The chemosensing mechanism

The weak basic character of both the tertiary aromatic amine and the azo groups of monomers (**3**) and (**4**) is responsible for the acidity sensing behaviour of the materials prepared herein (Scheme 3). Thus, the colour change visually observed for the materials when exposed to acidic media mainly arises from the protonation of these groups. It is this colour variation that permits the building of titration curves using the UV/vis technique as well as the qualitative visual determination of the acidity of the media using the naked eye.

The sensing mechanism has been analysed in terms of the deprotonation/protonation equilibrium of weak basic species. Quite notably, it is fairly unusual and uncommon to see studies that have been performed with these types of materials in the solid state both in air and immersed in water. The acrylic membrane **M1** is a gel material that swells in water, and the solvated hydronium ions can enter the water swelled membrane by diffusion, reaching the basic moieties of the pendant azobenzene derivative. Similarly, the low hydrated but hydrophilic nature of the thin polyamide films of **PA1** and **PA2** allow for the same diffusion and reaction processes. In addition, in a comparable fashion, these materials can be hydrated in air due to the ambient relative humidity, and HCl vapours can then be dissolved and transported into the membrane where the protonation processes occur. The deprotonation/protonation equilibria can be described by,

$$BH^+ \overset{K_1}{\rightleftharpoons} B + H^+$$

Scheme 3 Protonation sites on the sensory motif of films (each is marked with a pK label), which protonate upon increasing the acidity of the media. In water, pK_1 and pK_2 were observed for **M1** but only pK_1 for **PA1** (up to a perchloric acid concentration of 3 M). In gas phase, both pK_1 and pK_2 were observed for both **M1** and **PA1** (the pKs are shown in Table 4).

where the equilibrium constant is

$$K_1 = \frac{a_B a_{H^+}}{a_{BH^+}} \tag{1}$$

and eqn (1) can be rewritten as,

$$pK_1 = pH + \log\frac{[BH^+]}{[B]} - \log\frac{f_B}{f_{BH^+}} \tag{2}$$

where f represents the activity factors of the protonated species, BH^+, and free base, B. Considering an ionisation ratio, I, as the ratio between the concentration of the protonated species and free base and ideal behaviour of the solutions, *i.e.*, the activity coefficients are 1, eqn (2) can be written as,

$$\log I = -pH + pK_1 \tag{3}$$

However, eqn (3) allows for better results when expressed as[44,45]

$$\log I = -n_1 pH + n_1 pK_1 \tag{4}$$

where n_1 gives an idea of the lack of ideality of the system. Eqn (3) and (4) are the same for ideal systems where $n_1 = 1$. The ionisation ratio can be calculated from the absorbance values of UV/Vis measurements using eqn (5), which can be obtained from the mass and absorbance balance, where A_B, A_{BH^+} and A represent the absorbances of free base, protonated base, and the absorbance values at different pH for a given wavelength, λ, respectively. Substituting eqn (5) into (4), eqn (6) is obtained, which enables a nonlinear least squares fit of the sigmoid curve obtained from experimental measurements, known as the Chandler method.[46]
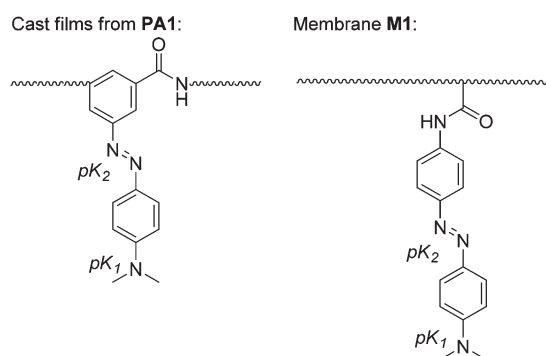
$$I = \left(\frac{A - A_B}{A_{BH^+} - A}\right)_\lambda \tag{5}$$

$$A = \frac{A_B - A_{BH^+}}{1 + 10^{-n_1 pH + n_1 pK_1}} + A_{BH^+} \tag{6}$$

The acidity necessary to fully protonate weak bases is such that the concentration of protons in the medium is greater than 0.1 M, and the pH as a measure of the acidity of the medium is not useful. Moreover, when operating at increasingly acidic medium, the ionic strength of the medium increases, making the approach used by Debye–Hückel increasingly unsatisfactory. It is therefore necessary to define a quantitative scale to express the acidity of the medium. For this reason Hammett and Deyrup proposed an acidity function,[47] H_0, representative of the acidity of the medium and independent of the nature of the indicator used as the reference in its definition and calculation. From a series of reference bases, S, the H_0 function is defined as:

$$H_0 = -\log\frac{a_{H^+}f_S}{f_{SH^+}} \tag{7}$$

If the base objects of study, B, fully or partially protonated in the acidic range in which the reference base is protonated,

S, according to Hammett's hypothesis, must meet the following conditions:

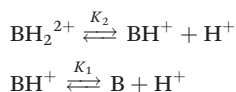$$\frac{f_S}{f_{SH^+}} = \frac{f_B}{f_{BH^+}} \tag{8}$$

H_0, in this case, depends only on the activity of protons because it is a measure of the acidity of the medium. Hammett and Deyrup calculated H_0 using a series of primary nitroanilines; their values are dependent only on the concentration of the mineral acid used. The correspondence of the calculated H_0 with the molar concentration of the acids used for this study, perchloric and hydrochloric acid, is shown in the ESI, Tables S1 and S2.†[48,49]

Following a similar reasoning to eqn (1) through (4), the corrected Hammett–Deyrup equation is proposed:[45,50]

$$\log I = -n_i H_0 + n_i \mathrm{p}K_i \tag{9}$$

Since the bases studied in this work are protonated in the high acidity region, in eqn (6), the pH is replaced by H_0 where needed, i.e., when the acid concentration is higher than 0.1 M.

Bases with two protonation equilibria, such as membrane **M1**, can be described with two equilibrium constants:

$$BH_2^{2+} \underset{}{\overset{K_2}{\rightleftharpoons}} BH^+ + H^+$$

$$BH^+ \underset{}{\overset{K_1}{\rightleftharpoons}} B + H^+$$

In this work, these two equilibria overlap, i.e., the difference between their pKs is less than or equal to three units, indicating that both processes cannot be separated. To determine the values of the equilibrium constants by UV/vis, different wavelengths, characteristic of each equilibrium constant, are required. In the event that this is not possible, it is necessary to propose an alternative approach.

From the ratio of ionisation of the two equilibria obtained from eqn (4), eqn (10) and (11) are obtained,

$$I_1 = \frac{[BH^+]}{[B]} = \left(\frac{a_{H^+}}{K_1}\right)^{n_1} \tag{10}$$

$$I_2 = \frac{[BH_2^{2+}]}{[BH^+]} = \left(\frac{a_{H^+}}{K_2}\right)^{n_2} \tag{11}$$

For convenience, the concentrations of B, BH$^+$ and BH$_2^{2+}$ are henceforth represented by C_1, C_2, and C_3, respectively. From a mass and absorbance balance, eqn (12) and (13) are obtained, where ε_1, ε_2 and ε_3 are, respectively, the molar extinction coefficients of B, BH$^+$ and BH$_2^{2+}$. Using eqn (10)–(12), eqn (14)–(16) are obtained.

$$C_T = C_1 + C_2 + C_3 \tag{12}$$

$$A = \varepsilon_1 C_1 + \varepsilon_2 C_2 + \varepsilon_3 C_3 \tag{13}$$

$$C_2 = C_1 K_1^{-n_1} a_{H^+}{}^{n_1} \tag{14}$$

$$C_3 = C_1 K_1^{-n_1} K_2^{-n_2} a_{H^+}{}^{n_1+n_2} \tag{15}$$

$$C_1 = \frac{C_T}{1 + K_1^{-n_1} a_{H^+}{}^{n_1} + K_1^{-n_1} K_2^{-n_2} a_{H^+}{}^{n_1+n_2}} \tag{16}$$

By substituting eqn (14)–(16) in (13), eqn (17) is obtained, where A_1, A_2 and A_3 represent the absorbance of species B, BH$^+$ and BH$_2^{2+}$, respectively. The activity of the proton can be replaced by $10^{-\mathrm{pH}}$ or 10^{-H_0}, depending on the acidity of the experiment, and K_i can be replaced by $10^{-\mathrm{p}K_i}$ in eqn (17). After performing a nonlinear least squares fit, this equation allows the attainment of the pKs, n_i and A_i, as previously described.[51]

$$A = \frac{A_1 + A_2 K_1^{-n_1} a_{H^+}{}^{n_1} + A_3 K_1^{-n_1} K_2^{-n_2} a_{H^+}{}^{n_1+n_2}}{1 + K_1^{-n_1} a_{H^+}{}^{n_1} + K_1^{-n_1} K_2^{-n_2} a_{H^+}{}^{n_1+n_2}} \tag{17}$$

The behaviour of the materials as proton receptors, i.e., as sensory materials for high acidity media, is both highly dependent on the nature of the receptor moiety and film or membrane constitution, and on the measuring media, i.e., the acidity in water or acid vapours, as shown in Tables 4 and 5. These results arise from the UV/vis titration curves depicted in Fig. 2 and 3 and in the ESI† (Fig. S9 and S10), and permit the design or tuning of the sensory materials for different applications and environments. Thus, for instance, the two protonation processes, in terms of pKs, of the N,N-dimethylamino and azo groups are 1.78 and −0.5 for the acrylic membrane **M1** in water and −1.48 and −3.89 under the slightly hydrated atmosphere corresponding to the vapour acidity measurements

Table 4 pKs of **M1** and **PA1** in water obtained from eqn (6) and (17). The values between brackets are the pKs calculated for monomers (**3**) and (**4**) using the program Marvin Suite[52]

Material		Calculated at				Average
		390 nm	418 nm	464 nm	499 nm	
M1	pK_1		1.69 ± 0.02	1.86 ± 0.02		1.78 ± 0.02 (3.58)
	n_1		1.01 ± 0.04	1.12 ± 0.07		1.06 ± 0.05
	pK_2	−0.4 ± 0.2	−0.54 ± 0.05		−0.5 ± 0.2	−0.5 ± 0.1 (0.11)
	n_2	0.45 ± 0.07	4 ± 2		1.1 ± 0.2	1.8 ± 0.8
		430 nm	550 nm			Average
PA1	pK_1	0.86 ± 0.04	0.98 ± 0.02			0.92 ± 0.03 (3.24)
	n	1.3 ± 0.1	1.5 ± 0.1			1.4 ± 0.1

Table 5 pKs of **M1** (assuming a 24% of water, by weight) and **PA1** (10% of water, by weight) in an atmosphere of HCl vapours obtained from eqn (6) and (17)

Material		Calculated at 555 nm			
M1	pK_1	−1.48			
	pK_2	−3.89			
		426 nm	461 nm	570 nm	Average
PA1	pK_1	−2.7 (−2.9, −2.5)[a]	−2.5 (−2.7, −2.2)[a]	−2.6 (−2.8, −2.3)[a]	−2.6 (−2.8, −2.3)[a]
	pK_2		−3.5 (−3.6, −3.5)		

[a] The data between brackets correspond to the water content of the film: 5%, left, and 15%, right.

(a 24% by weight of hydration was assumed, in accordance with the water sorption studies, for calculations). In the case of aramid films, only the protonation of the *N,N*-dimethylamino group was observed in water with a pK = 0.92; two processes in the acidity vapour measurements were observed with pK values of −2.6 and −3.5. For these calculations, a hydration of 10% was used and no drastically different results were obtained using a higher and lower water content assumption (Table 5).

The complex nature of the protonated azo group was previously described by Jaffé and Gardner.[37] In relation to the *cis–trans* isomerisation, the process has no influence in our study because we mainly work under ambient light and thermal conditions, where the *trans* isomer is the predominant species, which was observed in our UV/vis and ^{1}H NMR studies. This is because the *trans* to *cis* isomerisation occurs under UV irradiation, and the *cis* to *trans* isomerisation occurs under visible light along with heating. Simultaneously, the latter process is much faster, by one order or magnitude, as reported by Tang *et al.*[31] In addition, acidic media have a well-known highly catalytic effect when undergoing a *cis* to *trans* isomerisation.[36]

The proposed protonation processes were also confirmed by ^{1}H NMR. Thus, the behaviour of the polyamide model compound (**5**) and the acrylic monomer (**3**) in a CD$_3$CN–D$_2$O (1.3/0.7 mL) solution upon acidification with DCl was studied using this technique. The first protonation process of the *N,N*-dimethylamino group was clearly seen for both compounds. The acidity constants were calculated in a similar way for the solid film shaped sensory materials. Details of the calculations and results are depicted in the ESI, section S7.† Unfortunately, it was not possible to increase the acidity in the NMR experiments to see further protonation processes for the acrylic monomer (**3**) or for the model (**5**). The acidity constants, in terms of pKs, were in agreement with those of the solid materials in water considering that due to the insolubility of (**3**) and (**5**) in water, the medium was mainly organic and that these are discrete molecules with high mobility. However, the sensory motifs in polymeric films or membranes are chemically anchored to a polymer structure within the solid state and, hence, have a highly restricted mobility.

Interference study

The selectivity of the sensory materials as colorimetric acidity sensors were tested in the presence of a broad set of salts (NaCl, KCl, CuSO$_4$·5H$_2$O, Co(NO$_3$)$_2$·6H$_2$O, Al(NO$_3$)$_3$·9H$_2$O, Pb(ClO$_4$)$_4$, FeSO$_4$·7H$_2$O, LiCl, Zn(NO$_3$)$_2$·6H$_2$O, Hg(NO$_3$)$_2$·H$_2$O, and Ni(NO$_3$)$_2$·6H$_2$O). Thus, a solution of all these salts at a high concentration, 1×10^{-3} M of each, in 1 M aqueous HClO$_4$ was used in this study. The UV/vis spectra of **M1** were obtained by dipping **M1** into this solution and, in parallel, into a pure solution of 1 M HClO$_4$ in water (Fig. S14†). The spectra were fairly similar, and slight changes were ascribed to the change in the acidity caused by the acidic salts.

Reusing and stability of the sensory membranes in acidic media

The reusability of a material is a key parameter in its applicability both from sustainability and economy viewpoints. It is related to the material's chemical stability and reproducibility as well as to the recovery of the material.

Thus, sensory materials, **M1** and **PA1**, were subjected periodically to 10 cycles of immersions in highly acidic water (4 M HClO$_4$) followed by washing in pure water, without loss of performance and simultaneously with good reproducibility (Fig. 4). The study of **PA1** was performed using a thin film (1.87 μm) prepared from casting over a microscopic glass slide, which gave rise to an extremely short measuring-recovery cycle time of approximately 2 min; however, this process was approximately 17 min for **M1**, including a 2 min immersion in the acidic medium and a 15 min wash. The differences most likely arise mainly from the thickness differences that influence the diffusion processes (Fick's law).

Response time

Sensors have to be not only accurate, reliable, and resistant to the environment, but also rapid in their response for real live measurements; thus, response time is a key parameter for sensor performance. In this study, response time was determined by UV/vis spectroscopy as the time needed to achieve 99.8% of the absorbance variation (ESI, Fig. S13†). The colour change was immediate for polyamide films and lower than
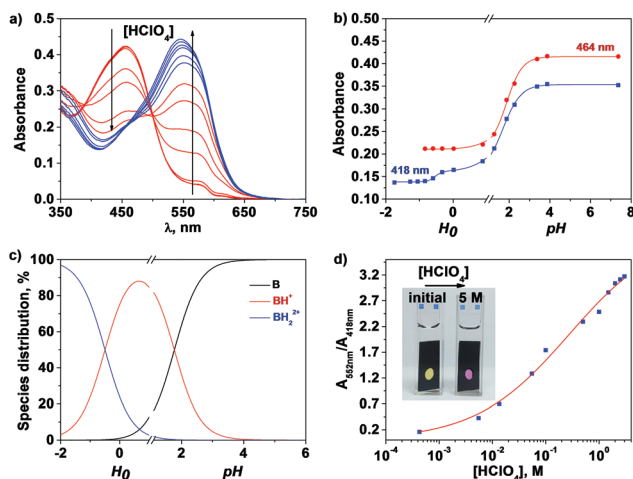
Fig. 2 Titration of perchloric acid with membrane **M1** in Millipore-Q water using the UV/Vis technique: (a) UV/Vis spectra showing the two protonation processes (lower and higher acidity in red and blue, respectively); (b) acidity absorbance relationship at 418 and 464 nm (continuous lines correspond to the fitting using eqn (17) and (6), respectively); (c) species distribution using eqn (10) and (11), assigning a value of 100 to C_T; (d) ratiometric titration curve of perchloric acid ([HClO$_4$] vs. absorbance at 552 and 418 nm ratio); inset: picture of the UV/vis cuvettes at the beginning and end of the experiment showing the colour change upon acidification of the medium.
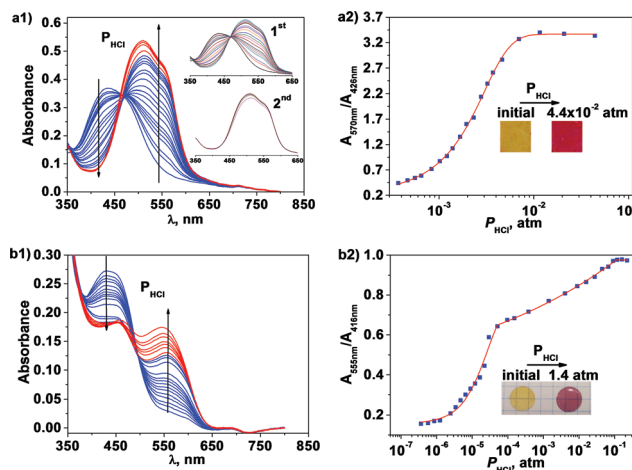

Fig. 3 Titration of HCl vapours with the cast film of **PA1** and membrane **M1**: (a1) **PA1**, UV/Vis spectra showing the two protonation processes (lower and higher acidity in blue and red, respectively) (inset: first and second processes at lower and higher acidity, respectively), (a2) **PA1**, ratiometric titration curve of HCl vapours, in terms of partial pressure, vs. absorbance at 570 and 462 nm ratio (inset: picture of the film at the beginning and end of the experiment showing the colour change upon increasing the partial vapour pressure of HCl); (b1) **M1**, UV/Vis spectra showing the two protonation processes (lower and higher acidity in blue and red, respectively); (b2) **M1**, ratiometric titration curve of HCl vapours, in terms of partial pressure, vs. absorbance at 555 and 416 nm ratio; inset: picture of the membrane at the beginning and end of the experiment showing the colour change upon increasing the partial vapour pressure of HCl.

3 min for the acrylic sensory membrane **M1**, and colour changes were clearly visible using only the naked eye in less than one minute. Fig. S13 in the ESI† also shows the stability of the measurement with time.

Sensing acidic aqueous media

The variation in the UV/vis spectra of membrane **M1** and polyamide cast films allowed for the construction of ratiometric titration curves as well as for the naked eye visualisation of increasing acidity, as shown in Fig. 2d and S9 (ESI†). **M1** shows a continuous change in the absorbance ratio at 552 and 418 nm (A_{552}/A_{418}) from a low perchloric concentration (4 × 10^{-4} M) to high acidities (3 M). On the other hand, films prepared with **PA1** show continuous variation in the A_{550}/A_{408} ratio in the medium acidity range (from 2 × 10^{-3} to 1 × 10^{-2} M) (Fig. S9 (ESI†)). This sensing range is in agreement with the acidity constant or constants of the materials discussed above.

Sensing acidic atmospheres

The detection and control of acids in the environment is important for health and safety at work, and also for environmental and industrial control. In this context, it is particularly important to be able to easily and quickly detect a visual signal that indicates the presence of an acidic atmosphere.[53,54] Within this frame, a 5 min exposure to hydrogen chloride gases of sensory film **PA1** and membrane **M1** turn the yellowish materials to red or purple. Moreover, similarly to aqueous media, a UV/vis ratiometric response was observed for partial HCl pressures ranging from 4 × 10^{-4} to 1 × 10^{-2} atm for the

former and from 4 × 10^{-7} to 9 × 10^{-2} atm for the latter (Fig. 3 and S10 (ESI†)).

On the other hand, a 5 min exposure to the acidic media turned both materials from yellow to red, clearly permitting the visual qualitative evaluation of the acidity of the media (Fig. 2d and S9 (ESI†)).

Smart fibres and fabrics as colorimetric acid sensors

Intelligent fabrics or smart labels made of smart fibres are promising materials for future and forthcoming applications as stand-alone systems in a number of advanced technological fields, such as sensors and actuators, energy storage tools, stimuli responsive materials, etc.[18,55–57]

Within this context, we believe that smart textiles capable of sensing acidic media with macroscopic colour changes as a signal are promising materials. In this line, the coating of commercial fibres is a simple and straightforward way of economically transforming these fibres into smart fibres without impairing the weaving and wearable characteristics of the fabrics prepared with them. Thus, we have coated commodity cotton fabrics and high-tech meta- and para-aramid fabrics and yarns with acrylic and aramid sensory coatings, with a weight percent coating ranging from 0.4 to 1.6% in the case of the aramid and from 96 to 674% for the acrylic coatings. These coated yarns and fabrics changed their colour clearly upon exposure to HCl vapour from orange to pink-red for the
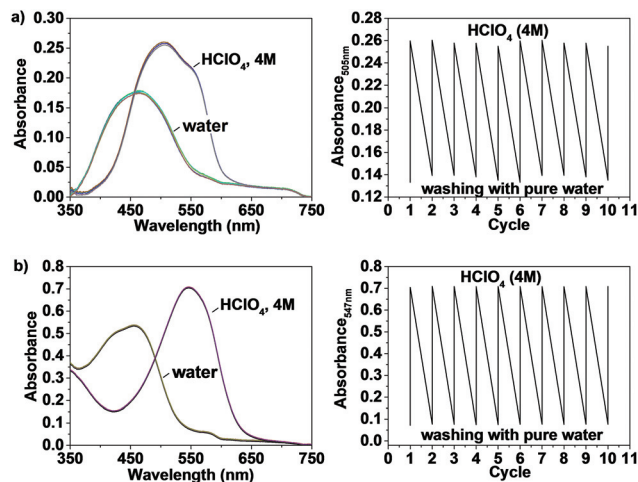
Fig. 4 Reproducibility and reversibility of **M1** (b) and cast films of **PA1** (a) on a glass surface as acidity sensors analysed by UV/vis spectroscopy (left: UV/vis spectra; right: absorbance *vs.* measuring cycle). The measurements were performed by successive cycles of dipping the material in highly acidic water (4 M HClO₄), followed by washing with pure water. The measuring-recovery cycle time was approximately 17 min for **M1**, which included a 2 min immersion in the acidic medium and a 15 min wash, and approximately 2 min for **PA1**, which included a 2 min immersion in the acidic medium, and the recovery was immediate after washing.

aramid coating and to dark purple in the case of the acrylic coating, as depicted in Table 1.

Conclusions

Colorimetric sensory polymers sensitive toward acidic media, both in water and in the environment, have been designed and transformed or synthesised into manageable films or membranes, or even as acid-responsive commodity and high-tech textiles that change their colour upon contact with an acidic aqueous atmosphere. These sensory materials are reusable; the materials are recovered by washing with water and are highly stable under acidic conditions for long periods of time. The polymeric materials were both aromatic polyamides and an acrylic network with gel behaviour. The polymers have covalently bonded conjugated azo groups and amino moieties in their pendant structure: the former as a colorimetric moiety and a weak basic motif, and the latter also as a weak, but stronger, basic group and simultaneously as an electron donor or electron withdrawal group in its non-protonated and protonated forms. The pK_as of the protonisable groups were different for the various polymers and also for the measurements in water and in air, and allowed for the detection of acidic media in water ranging from a concentration of perchloric acid of 1×10^{-2} to 3 M, and in air ranging from a vapour pressure of hydrogen chloride from 4×10^{-7} to 9×10^{-2} atm. Accordingly, the envisaged application includes intelligent textiles and tags for use in health and safety at work, along with

applications for acidity control in industrial processes and laboratories and in the environment.

Notes and references

1 R. G. Bates, *Determination of pH: Theory and Practice*, Wiley-Interscience, New York, 2nd edn, 1973.
2 D. Wencel, T. Abel and C. McDonagh, Optical Chemical pH Sensors, *Anal. Chem.*, 2014, **86**, 15–29.
3 Z. Jin, Y. Su and Y. Duan, *Sens. Actuators, B*, 2000, **71**, 118–122.
4 H.-X. Chen, X.-D. Wang, X.-H. Song, T.-Y. Zhou, Y. Q. Jiang and X. Chen, *Sens. Actuators, B*, 2010, **146**, 278–282.
5 D. K. Nordstrom, C. N. Alpers, C. J. Ptacek and D. W. Blowes, Negative pH and Extremely Acidic Mine Waters from Iron Mountain, California, *Environ. Sci. Technol.*, 2000, **34**, 254–258.
6 K. J. Kuhn and J. T. Dyke, *Anal. Chem.*, 1996, **68**, 2890–2896.
7 M. Shamsipur and G. Azimi, *Anal. Lett.*, 2001, **34**, 1603–1616.
8 W. P. Carey and M. D. DeGrandpre, *Anal. Chem.*, 1989, **61**, 1674–1678.
9 L. R. Allain, K. Sorasaenee and Z. Xue, *Anal. Chem.*, 1997, **69**, 3076–3080.
10 M. H. Noiré, L. Couston, E. Douarre and D. Pouy, *J. Sol-Gel Sci. Technol.*, 2000, **17**, 131–136.
11 J. M. García, F. C. García, F. Serna and J. L. de la Peña, *Prog. Polym. Sci.*, 2010, **35**, 623–686.
12 K. Marchildon, *Macromol. React. Eng.*, 2011, **5**, 22–54.
13 M. Trigo-López, J. L. Pablos, F. C. García, F. Serna and J. M. García, *J. Polym. Sci., Part A: Polym. Chem.*, 2014, **52**, 1469–1477.
14 M. Trigo-López, J. L. Barrio-Manso, F. Serna, F. C. García and J. M. García, *Macromol. Chem. Phys.*, 2013, **214**, 2223–2223.
15 S. Vallejos, A. Muñoz, S. Ibeas, F. Serna, F. C. García and J. M. García, *J. Mater. Chem. A*, 2013, **1**, 15435–15441.
16 J. L. Pablos, M. Trigo-López, F. Serna, F. C. García and J. M. García, *Chem. Commun.*, 2014, **50**, 2484–2487.
17 S. Vallejos, A. Munoz, S. Ibeas, F. Serna, F. C. García and J. M. García, *J. Hazard. Mater.*, 2014, **276**, 52–57.
18 J. L. Pablos, M. Trigo-López, F. Serna, F. C. García and J. M. García, *RSC Adv.*, 2014, **4**, 25562–25568.
19 O. Korostynska, K. Arshak, E. Gill and A. Arshak, *Sensors*, 2007, **7**, 3027–3042.

20 T. A. Canada, L. R. Allain, D. B. Beach and Z. Xue, *Anal. Chem.*, 2002, **74**, 2535–2540.

21 Y. Tian, E. Fuller, S. Klug, F. Lee, F. Su, L. Zhang, S. Chao and D. R. Meldrum, *Sens. Actuators, B*, 2013, **188**, 1–10.

22 U.-W. Grummt, A. Pron, M. Zagorska and S. Lefrant, *Anal. Chim. Acta*, 1997, **357**, 253–259.

23 Q.-J. Ma, H.-P. Li, F. Yang, J. Zhanga, X.-F. Wu, Y. Bai and X.-F. Li, *Sens. Actuators, B*, 2012, **166–167**, 68–74.

24 P. Hashemi and R. A. Zarjani, *Sens. Actuators, B*, 2008, **135**, 112–115.

25 D. Wencel, B. D. MacCraith and C. McDonagh, *Sens. Actuators, B*, 2009, **139**, 208–213.

26 Y. Kostov and S. Tzonkov, *Anal. Chim. Acta*, 1993, **280**, 15–19.

27 S. Blair, M. P. Lowe, C. E. Mathieu, D. Parker, P. K. Senanayake and R. Kataky, *Inorg. Chem.*, 2001, **40**, 5860–5867.

28 A. Lobnik, I. Oehme, I. Murkovic and O. S. Wolfbeis, *Anal. Chim. Acta*, 1998, **367**, 159–165.

29 A. A. Ensafi and A. Kazemzadeh, *Microchem. J.*, 1999, **63**, 381–388.

30 S. Capel-Cuevas, M. P. Cuéllar, I. de Orbe-Payá, M. C. Pegalajar and L. F. Capitán-Vallvey, *Microchem. J.*, 2011, **97**, 225–233.

31 Q. Tang, X. Meng, H. Jiang, T. Zhou, C. Gong, X. Fu and S. Shi, *J. Mater. Chem.*, 2010, **20**, 9133–9139.

32 N. Feng, G. Han, J. Dong, H. Wu, Y. Zheng and G. Wang, *J. Colloid Interface Sci.*, 2014, **421**, 15–21.

33 L. Chen, S.-G. Li, Y.-P. Zhao, Y.-C. Wang and Q.-W. Wang, *J. Appl. Polym. Sci.*, 2005, **96**, 2163–2167.

34 A. M. Sanchez and R. H. de Rosi, *J. Org. Chem.*, 1995, **60**, 2974–2976.

35 A. M. Sanchez and R. H. de Rosi, *J. Org. Chem.*, 1996, **58**, 2094–2096.

36 S. Ciccone and J. Halpern, *Can. J. Chem.*, 1959, **37**, 1903–1910.

37 H. H. Jaffé and R. W. Gardner, *J. Am. Chem. Soc.*, 1958, **80**, 319–322.

38 I. M. Klotz, H. A. Fiess, J. Y. Chen Ho and M. Mellody, *J. Am. Chem. Soc.*, 1954, **76**, 5136–5140.

39 S. Miao, H. Li, Q. Xu, N. Li, J. Zheng, R. Sun, J. Lu and C. M. Lic, *J. Mater. Chem.*, 2012, **22**, 16582–16589.

40 C. D. Diakoumakos and J. A. Mikroyannidis, *J. Appl. Polym. Sci.*, 1998, **64**, 921–930.

41 D. Ramachandran, C. C. Corten and M. W. Urban, *RSC Adv.*, 2013, **3**, 9357–9364.

42 J. L. Barrio-Manso, P. Calvo, F. C. García, J. L. Pablos, T. Torroba and J. M. García, *Polym. Chem.*, 2013, **4**, 4256–4264.

43 J. L. Pablos, P. Estévez, A. Muñoz, S. Ibeas, F. Serna, F. C. García and J. M. García, *J. Mater. Chem. A*, 2015, **3**, 2833–2843.

44 B. García and J. M. Leal, *Collect. Czech. Chem. Commun.*, 1987, **52**, 299–307.

45 B. García and J. C. Palacios, *Ver. Bunsen. Phys. Chem.*, 1998, **92**, 696–700.

46 W. D. Chandler and D. G. Lee, *Can. J. Chem.*, 1990, **68**, 1757–1761.

47 L. Hammett and A. J. Deyrup, *J. Am. Chem. Soc.*, 1932, **54**, 2721–2739.

48 K. Yates and H. Wai, *J. Am. Chem. Soc.*, 1964, **86**, 5408–5413.

49 R. A. Cox, *Adv. Phys. Org. Chem.*, 2000, **35**, 1–66.

50 B. García, J. M. Leal, J. C. Palacios and L. A. Herrero, *J. Chem. Soc., Perkin Trans. 2*, 1988, 1759–1768.

51 B. García, F. Secco, S. Ibeas, A. Muñoz, F. J. Hoyuelos, J. M. Leal, M. L. Senent and M. Venturini, *J. Org. Chem.*, 2007, **72**, 7832–7840.

52 Marvin Suite software, ver. 6.2.1, ChemAxon Ltd (http://www.chemaxon.com), 2014.

53 D. S. Ballantine Jr. and D. Callahan, *Talanta*, 1992, **39**, 1657–1667.

54 M. G. Baron, R. Narayanaswamy and S. C. Thorpe, *Sens. Actuators, B*, 1996, **34**, 511–515.

55 L. Van Langenhove, C. Hertleer and A. Schwarz, Smart Textiles: An Overview, in *Intelligent Textiles and Clothing for Ballistic and NBC Protection, NATO Science for Peace and Security Series B: Physics and Biophysics*, ed. P. Kiekens and S. Jayaraman, Springer, Dordrecht, 2012, ch. 6, pp. 119–136.

56 P. Westbroek, G. Priniotakis and P. Kiekens, Intelligent/smart materials and textiles: an overview, in *Analytical electrochemistry in textiles*, Woodhead Publishing Limited and CRC Press LLC, Cambridge, 2005, ch. 8, pp. 215–243.

57 K. Cherenack and L. van Pieterson, *J. Appl. Phys.*, 2012, **112**, 091301.